Robust Fetal Heart Rate Tracking through Fetal Electrocardiography (ECG) and Photoplethysmography (PPG) Fusion *

Begum Kasap, Kourosh Vali, Weitai Qian, Mahya Saffarpour, Randall Fowler, and Soheil Ghiasi

Abstract—Fetal electrocardiogram (fECG) or photoplethysmogram (fPPG) devices are being developed for fetal heart rate (FHR) monitoring. However, deep tissue sensing is challenged by low fetal signal-to-noise ratio (SNR). Data quality is easily degraded by motion, or interference from maternal tissues and data losses can happen due to communication faults. In this paper, we propose to combine fECG and fPPG measurements in order to increase robustness against such dynamic challenges and increase FHR estimation accuracy. To the author's knowledge the fusion of two sensory data types (fECG, fPPG) has not been investigated for FHR tracking purposes in the literature. The proposed methods are evaluated on real-world data captured from gold-standard large pregnant animal experiments. A particle filtering algorithm with sensor fusion in the measurement likelihood, called KUBAI, is used to estimate FHR. Fusion of PPG&ECG data resulted in 36.6% improvement in root-mean-square-error (RMSE) and 20.3% improvement in R^2 correlation between estimated and reference FHR values compared to single sensor-type (PPG-only or ECGonly) data. We demonstrate that using different types of sensory data improves the robustness and accuracy of FHR tracking.

I. INTRODUCTION

The primary signal used in antenatal monitoring is fetal heart rate (FHR). Physicians use cardiotocography (CTG) to observe FHR together with the mother's uterine contractions to assess fetal health [1]. However, CTG is easily disturbed by fetal movements and maternal breathing. Thus, frequent adjustment to the transducer placement is needed, disrupting continuous monitoring [2].

In addition to CTG, wearable devices capturing fetal electrocardiogram (ECG) or photoplethysmogram (PPG) have emerged over the past few years. The fetal ECG (fECG) technology involves placing specialized electrodes on the maternal abdomen to pick up the electrical signals produced by the fetal heart [3]. fECG can be used to detect conditions such as fetal arrhythmia and congenital heart defects [4].

Transabdominal fetal pulse oximetry (TFO) is a non-invasive technique used to measure the oxygen saturation of fetal blood through captured PPG signals [5]–[8]. It involves the use of an optical probe (optode) that is placed on the maternal abdomen. The optode emits near-infrared (NIR) light, and the reflected light is captured using photodetectors [9]. TFO can be used to detect fetal hypoxia [10].

*This work was supported by the National Science Foundation (NSF) under Grants IIS-1838939, CCF-1934568; the National Institutes of Health (NIH) under Grant 5R21HD097467, and the National Center for Interventional Biophotonic Technologies through NIH Grant 1P41EB032840.

B. Kasap, K. Vali, W. Qian, M. Saffarpour, R. Fowler and S. Ghiasi are with the Electrical & Computer Engineering Department, University of California Davis, Davis, CA 95616, USA (e-mail: bkasap@ucdavis.edu)

Both fetal ECG and TFO are still under development and further research is needed to improve their accuracy and reliability in estimating FHR. Targeted fetal signal in deep-tissue sensing is challenged by the low signal-to-noise ratio (SNR). Data quality is easily degraded by bad sensor placement, motion and different unwanted signals from the sensed medium and signals could be even lost due to communication faults. In this paper, we propose to combine fECG and TFO's PPG measurements through sensor fusion in order to increase robustness against such dynamic challenges and increase FHR estimation accuracy. The proposed methods are evaluated on real-world data captured from gold-standard large pregnant animal experiments.

II. METHODS

A. Fetal PPG (fPPG)

Fetal PPG (fPPG) signals are collected using reflectance based pulse oximetry. Transabdominal fetal pulse oximeter (TFO) is a novel, non-invasive device that uses two NIR LEDs, and 5 photodetectors to estimate fetal oxygenation through captured PPG waveforms [9].

As light source-detector distance increases on TFO, the captured photons at the mother's abdominal surface are more likely to have reached the depths of the fetus [9], as illustrated in Fig. 1b. The optical probe (optode) with the LED and photodetectors is shown in Fig. 1a. The closest detector D1 to the LED, mostly captures maternal PPG, and a very faint fetal PPG only in subjects with shallow fetal depth. The further photodetectors, D2 to D5, collect a mixture of maternal and fetal PPG [9], [11].

The fetus is located a few centimeters deep from the maternal abdomen's surface, where the TFO is placed. Thus, the mixed PPG signals contain a very strong maternal noise and a very weak fetal signal. Maternal noise refers to maternal heart rate (MHR), maternal respiration rate (MRR) and Mayer waves [6]. Motion is also a major source of noise. The fPPG needs to be filtered and processed to compute FHR. Researchers have reported adaptive filtering can expose the weak fPPG from TFO's measurements [11], [12].

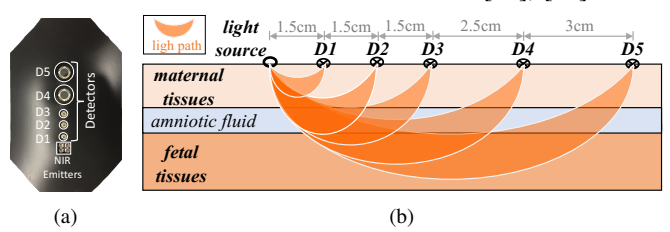


Fig. 1: (a) Picture of optical probe (optode) [11]. (b) Illustration of light path through maternal and fetal tissues and reflected back to the optode.

B. Fetal ECG (fECG)

The ECG signal of a fetal heart is monitored by electrodes placed on the mother's abdomen to create a fetal ECG (fECG) [3]. fECG uses the same principle as the adult ECG, but it is much lower in amplitude due to weak fetal cardiac potential and poor conductivity layers around the fetus. There also exists high interference from surrounding tissue, such as maternal ECG, maternal respiration, and motion artifacts [4].

Many different electrode counts and placements have been researched to capture fECG. As electrode count increases, researchers have reported higher FHR tracking accuracy [4]. However, we are constrained by the maternal abdomen's surface area. As we want to have both the TFO device and ECG electrodes placed simultaneously, we choose to use a 5electrode configuration [3], [4]. There exists a commercially available portable fetal ECG device, Monica AN24, that uses 5 electrodes to capture 3 channels of fECG. Therefore, the placement of the electrodes is adapted from the user manual of Monica AN24 [13]. The reference (-) electrode is placed on the fetal head, with 3 (+) channels placed around its body.

Similar to fPPG, fECG signals need to be filtered and processed before estimating the FHR. The challenges in fECG are very similar to those in fPPG as both are noninvasive deep-tissue sensing modalities. Past research has found merit in using adaptive filtering to isolate fECG [14].

C. In Vivo Data Acquisition

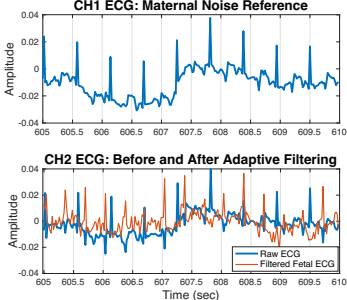
The dataset used in this paper is gathered from gold standard hypoxic lamb model. The institutional animal care and use committee (IACUC) at UC Davis approved the study protocol, which was adhered to in all operations. Fetal hypoxia is progressively induced by inserting an aortic occlusion balloon catheter into three nearly-term ewes, and by controlling the blood flow to the femoral artery. Through the use of hemodynamics and an arterial line placed into the fetus' neck, reference FHR data was collected. Reference maternal heart rate (MHR) numbers were also measured through hemodynamics. These experiments were conducted to test TFO's ability to accurately estimate fetal oxygen saturation and more details can be found in [7], [15].

TFO PPG data is collected using a custom data acquisition system at a sampling rate of 8kHz. Reference FHR and MHR values are recorded using BIOPAC. In addition to TFO, ECG electrodes are secured in place on the ewe's abdomen around the TFO optode. Fig. 2 shows a picture from an experiment, where the placement of the electrodes and the TFO optode can be seen. 3 channels of ECG data are collected using BIOPAC ECG100C amplifiers with a gain of 5000, highpass and low-pass filters at [0.05Hz, 35Hz], and a sampling rate of 500Hz.

D. Fetal Heart Rate Tracking

1) Data Processing: Maternal waves and motion can mask the fetal PPG and ECG measurements, causing wrong FHR estimation. Thus, the captured data is passed through multiple processing steps, visualized in Fig. 4. These steps have been adapted from previous research [16].





of ECG electrodes and TFO optode on the ewe's abdomen.

Fig. 2: Photo showing placement Fig. 3: Result of Adaptive Noise Cancellation applied to CH2 to filter fetal ECG in time-domain.

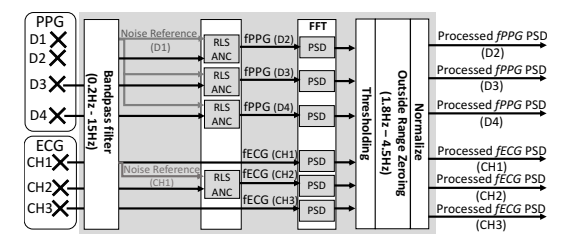


Fig. 4: Block diagram of data processing steps.

First, PPG and ECG data are downsampled to 50Hz. Next, a band-pass filter ([0.2Hz, 15Hz]) is applied to time-series PPG and ECG data to remove low and high-frequency noise. Then, to remove maternal PPG and ECG from the captured data, we apply recursive-least-squares (RLS) adaptive noise cancellation (ANC). The maternal noise reference is TFO detector D1 data for PPG. ANC is applied to all further detectors in TFO. Examples of noise-canceled fPPG can be found in [11].

When applying ANC to ECG data, CH1 is used as the maternal noise reference. Only CH2 ECG is passed through ANC. Because, we have observed that CH3 electrode already captured a trace that is not dominated by maternal ECG, and does not need ANC to expose fECG. Fig. 3 shows the result of ANC applied to CH2 ECG data. The baseline wandering in raw ECG data is due to maternal respiration. The raw and filtered ECG have fetal R peaks in opposite directions due to electrode placement. The Raw ECG signal has been reversed to have positive maternal R peaks in Fig. 3.

Since our goal is to extract the FHR, which is a periodic signal, it is easier to track it in frequency domain. We compute power spectral densities (PSD) of PPG and ECG data using Hanning windows of 30 seconds with 50% of overlap. All spurious peaks within FHR range are zeroed-out through thresholding. All peaks outside the FHR range (110 -270 beats-per-minute (BPM)) are multiplied by zero as well. Finally, all processed PSDs are normalized to have an area equal to 1 [16]. fPPG and fECG PSDs processed through these steps are visualized as Spectrograms (PSD over time) in Fig. 5, for the entire duration of an experiment.

2) Particle Filtering and KUBAI: In the literature, particle filtering has been applied to TFO PPG data for FHR tracking, reporting promising results, and the resulting algorithm is named KUBAI [16]. Particle filtering is a stochastic algorithm that addresses well the dynamic challenges faced in

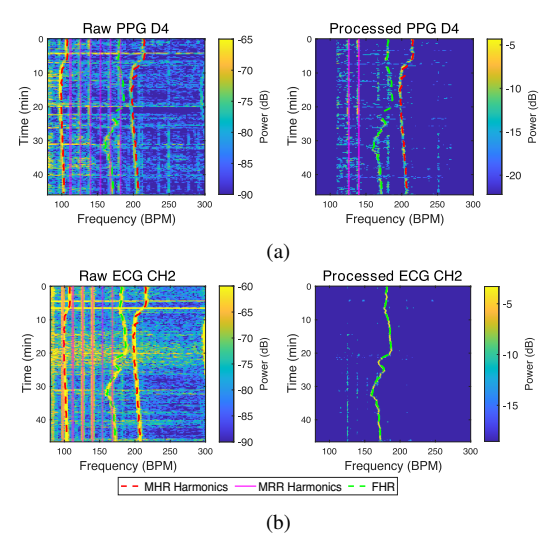


Fig. 5: Example spectrogram of data processing results for (a) PPG from D4 of TFO. (b) ECG from CH2 electrode.

FHR tracking from non-invasive measurements. For more details please refer to [16]. In this paper, we use KUBAI, tune its parameters, and apply it to both PPG and ECG data.

In [16], KUBAI outputs an FHR estimate every second while measurements are available every 30 seconds. We modify KUBAI such that FHR estimate is outputted only when a processed PSD is available every 15 seconds. The prior distribution $p(\widehat{FHR}_t^{(i)}|\widehat{FHR}_{t-1}^{(i)})$, representing how FHR prediction per particle $\widehat{FHR}_t^{(i)}$ moves over time, needs to be adjusted. Since FHR is expected to vary more within 15 seconds compared to 1 second, the variance of KUBAI's prior distribution is increased. $p(\widehat{FHR}_t^{(i)}|\widehat{FHR}_{t-1}^{(i)})$ is defined as a mixture of a Gaussian with an increased variance of $\sigma^2 = 10BPM^2$ and a Poisson motion with a rate $\lambda = 0.1BPM$.

3) Sensor Fusion: As each particle i makes an FHR estimate $\widehat{FHR}_t^{(i)}$ over time t, we assign a weight per particle depending on how good the particle's FHR estimate is. In the literature, KUBAI fuses processed TFO PPG measurements when computing the measurement likelihood $p(Meas_t|\widehat{FHR}_t^{(i)}, MHR_t)$, which directly affects the particle weights $\tilde{W}_t^{(i)}$, given in eq. (1) [16].

$$\widetilde{W}_{t}^{(i)} = \widetilde{W}_{t-1}^{(i)} * p(Meas_{t}|\widehat{FHR}_{t}^{(i)} MHR_{t})$$
 (1)

We have access to measurements from multiple sensors, supplying processed PPG and ECG data, that can be used to define the measurement likelihood $p(Meas_t|\widehat{FHR}_t^{(i)}, MHR_t)$. A function $f_{reward}(Meas_t|\widehat{FHR}_t^{(i)}, MHR_t)$ to reward each particle estimate $\widehat{FHR}_t^{(i)}$ is first defined using k individual measurement sources $f_{reward}(Meas_t|\widehat{FHR}_t^{(i)}, MHR_t)$, then fused through weighted-sums approach, as seen in eq. (2), where λ_k is the weight per measurement k [16]. λ_k should be chosen based on the expected reliability of each measurement channel to supply a good fetal signal. Finally, the measurement likelihood is defined as a Sigmoid of the total reward function, as shown in eq. (3) [16].

$$f_{reward}(Meas_{t}|\widehat{FHR}_{t}^{(i)}, MHR_{t}) = \sum_{k=1}^{K} \lambda_{k} * f_{reward}^{(k)}(Meas_{t}^{(k)}|\widehat{FHR}_{t}^{(i)}, MHR_{t})$$

$$p(Meas_{t}|\widehat{FHR}_{t}^{(i)}, MHR_{t}) = \frac{1}{1 + exp\left(\alpha\left(-f_{reward} + \beta\right)\right)}$$
with $\alpha = 470, \beta = 4.9e - 3$ (3)

III. RESULTS AND DISCUSSION

In the literature, KUBAI has been only applied to PPG data, and measurements from different detectors on TFO were used for sensor fusion [16]. We propose to supply KUBAI with the additional ECG data that was captured during in vivo experiments. By doing so, we aim to increase the accuracy of FHR estimation and also robustness against signal losses that can happen in a single sensor-type. For benchmarking purposes, we first input either PPG or ECG data to KUBAI, and compute measurement likelihood (3) by fusion of same sensor-type data channels.

All 3 fECG channels are used in FHR tracking, and only D2, D3, and D4 fPPG data are used. This is to have an equal number of channels per sensor-type, and as a result, make a fair comparison between PPG-only, ECG-only, and combined PPG&ECG FHR tracking accuracy. When PPG data from detectors $\{D2,D3,D4\}$ is used, the weight λ_k per detector is defined as $\{(2,3,3)/8\}$ respectively. Similarly, for ECG channels $\{CH1,CH2,CH3\}$, the weights are set to $\{(1,3,3)/7\}$. When both PPG&ECG data are input to KUBAI, the weights are adjusted as $\{(2,3,3;1,3,3)/15\}$ to keep the sum of weights equal to 1.

Root-mean-square error (RMSE) is used as the measure of accuracy for estimating FHR through the modified KUBAI algorithm. The average RMSE across 10 runs of the algorithm is reported to account for stochastic nature of KUBAI and change in FHR estimates for different runs $\widehat{FHR}_{t,r}$. Table I summarizes the results of FHR estimation with different sensor inputs. We notice that FHR tracking using ECG-only or PPG-only results in an overall similar RMSE.

Fig. 6 shows the distribution of overall RMSE for 10 runs of KUBAI with different sensor inputs. In Fig. 6, we notice that FHR tracking using ECG data results in a slightly lower median and a much smaller interquartile range (IQR) compared to PPG. This means ECG-based FHR estimates were similar across the 10 runs of KUBAI. However, the 25th percentile of ECG-only FHR detection is much higher than it's PPG-only counterpart. This means that ECG-only estimates tracked the wrong signal more consistently. Fig. 7 shows the linear regression analysis between estimated and reference FHR values. The R^2 correlation of FHR estimates, obtained from ECG-only inputs results in a low correlation of 0.33 with reference, while estimates obtained from PPG-only inputs result in a moderate correlation of 0.59.

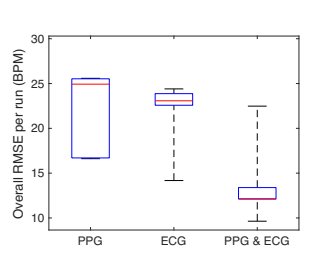
TABLE I: Fetal Heart Rate Estimation Performance Summary over 10 Runs Single Sensor-Type Fusion vs. Two Sensor-Type Fusion

Experiment	# of Estimations (N)	Mean RMSE (BPM) ¹			STDEV of RMSE (BPM) ²		
Experiment		PPG	ECG	PPG&	PPG	ECG	PPG&
				ECG			ECG
1	169	14.93	9.11	1.75	20.00	6.14	0.32
2	178	18.61	40.47	13.56	18.32	11.02	16.00
3	185	16.69	19.80	17.37	0.1	3.32	0.06
4	159	21.45	20.42	19.67	0.12	1.03	5.22
5	178	26.28	1.03	1.03	0.21	0.01	0.004
6	65	2.22	1.02	1.08	0.64	0.03	0.05
Overall	934	21.84	22.30	13.85	4.41	2.96	4.45

Maximum RMSE (BPM) ³						
PPG	ECG	PPG& ECG				
110	ECG					
44.15	14.27	2.55				
45.08	44.09	44.09				
16.51	23.19	17.42				
21.63	22.23	25.65				
26.58	1.05	1.03				
3.33	1.07	1.17				
45.08	44.09	44.09				

 ${}^{1} Mean(RMSE) = \frac{\sum_{r=1}^{10} \sqrt{\sum_{t=1}^{N} (FHR_{t} - \widehat{FHR}_{t,r})^{2}/N}}{10} \quad {}^{2} Stdev(RMSE) = \sqrt{\frac{\sum_{r=1}^{10} (RMSE_{r} - Mean(RMSE))^{2}}{10}} \quad {}^{3} Max(RMSE) = \sqrt{\frac{\sum_{r=1}^{10} (RMSE_{r} - Mean(RMSE))^{2}}{10}} \quad {}^{3} Max(RMSE_{r} - Mean(RMSE))} \quad {}^{3} Max(RMSE_{r} - Mean(RMSE)) = \sqrt{\frac{\sum_{r=1}^{10} (RMSE_{r} - Mean(RMSE))^{2}}{10}} \quad {}^{3} Max(RMSE_{r} - Mean(R$

 $^{3}Max(RMSE) = Max(RMSE_{r,expt})$



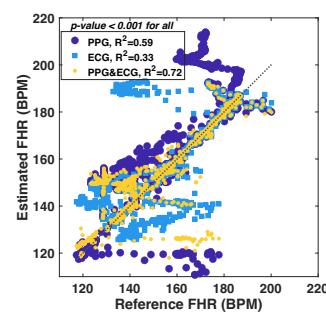


Fig. 6: Boxplots of estimated FHR RMSE overall in 6 experiments (10 algorithm runs), for different sensor inputs.

Fig. 7: Scatter plot of average FHR Estimates over the 10 runs vs. Reference, for different sensor inputs.

Fusing both sensor inputs, PPG&ECG, enables further improvement to FHR estimation performance. The distribution of PPG&ECG combined FHR estimation RMSE has the lowest percentiles and median, as seen in Fig. 6. Furthermore, we observe a high R^2 correlation of 0.72 between FHR estimates and reference when both PPG&ECG data are fused in KUBAI. This is a 20.3% improvement in correlation compared to PPG-only data input. Moreover, overall the RMSE of FHR estimates using PPG&ECG is 36.6% lower than using PPG-only data, as seen in Table I.

Let's analyze how combining two sensor types help with KUBAI's FHR estimation performance. In experiments 1, combining PPG&ECG helped KUBAI track FHR more consistently across the 10 runs, which in turn reduced the mean, Max and stdev of RMSE reported in Table I. The consistency is also visible from the smaller and lower IQR in Fig. 6.

In experiments 3 and 4, unfortunately, both PPG-only and ECG-only tracked MHR mostly instead of FHR and this does not change when using PPG&ECG data combined. It is important to note that experiments 3 and 4 present a case where the ECG amplifier connected to CH1 experienced communication faults. This in return degraded ANC's performance in extracting fECG in CH2 and caused a strong presence of maternal ECG in the signals input to KUBAI.

In experiment 5, ECG-only FHR tracking outperformed the PPG performance. Thus, the high accuracy of combined PPG&ECG output is thanks to the high-quality ECG data.

This demonstrates the importance of having different types

of sensors, to avoid losing accuracy due to data losses caused by device failure, or noise sources that can happen in a single sensor type. Using different types of sensor data in FHR tracking improves both robustness against unforeseeable dynamics and the accuracy of our algorithm's estimates.

REFERENCES

- Z. Alfirevic et al., "Continuous cardiotocography (CTG) as a form of electronic fetal monitoring (EFM) for fetal assessment during labour," Cochrane Database Systematic Reviews, 2017.
- [2] B. Karlsson et al., "Effects of fetal and maternal breathing on the ultrasonic doppler signal due to fetal heart movement." Eur. J. Ultrasound, vol. 11, no. 1, pp. 47–52, 2000.
- [3] N. Marchon, G. Naik, and R. Pai, "ECG electrode configuration to extract real time FECG signals," *Procedia Comp. Sci.*, vol. 125, pp. 501–508, 2018
- [4] G. Aggarwal and Y. Wei, "Non-invasive fetal electrocardiogram monitoring techniques: Potential and future research opportunities in smart textiles," *Signals*, vol. 2, no. 3, pp. 392–412, 2021.
- [5] A. Zourabian et al., "Trans-abdominal monitoring of fetal arterial blood oxygenation using pulse oximetry," J. Biomed. Opt., vol. 5, no. 4, pp. 391–405, 2000.
- [6] D. Fong et al., "Design and in vivo evaluation of a non-invasive transabdominal fetal pulse oximeter," *IEEE Trans. Biomed. Eng.*, vol. 68, no. 1, pp. 256–266, 2020.
- [7] K. Vali et al., "Estimation of fetal blood oxygen saturation from transabdominally acquired photoplethysmogram waveforms," in 43rd Int. Conf. IEEE Eng. Med. Biol. Soc., 2021, pp. 1100–1103.
- [8] B. Kasap et al., "Use of a novel transabdominal fetal pulse oximeter (TFO) in human pregnancy: A proof-of-concept," Amer. J. Obstet. Gynecol., vol. 228, no. 1, p. S100, 2023.
- [9] D. Fong et al., "Optode design space exploration for clinically-robust non-invasive fetal oximetry," ACM Trans. Embed. Comput. Syst., vol. 18, no. 5, pp. 1–22, 2019.
 [10] B. Kasap et al., "Towards Noninvasive Accurate Detection of Intra-
- [10] B. Kasap et al., "Towards Noninvasive Accurate Detection of Intrapartum Fetal Hypoxic Distress," in *IEEE 17th Int. Conf. Wearable Implantable Body Sensor Netw.*, 2021, pp. 1–4.
- [11] B. Kasap et al., "Multi-detector heart rate extraction method for transabdominal fetal pulse oximetry," in 43rd Int. Conf. IEEE Eng. Med. Biol. Soc., 2021, pp. 1072–1075.
- [12] K. B. Gan, E. Zahedi, and M. A. M. Ali, "Application of adaptive noise cancellation in transabdominal fetal heart rate detection using photoplethysmography," in *Adaptive Filtering Applications*, L. Garcia, Ed. Rijeka, Croatia: IntechOpen, 2011, ch. 6.
- [13] Monica AN24 Reference Operator Manual, Monica Healthcare, 2007.
- 14] A. Matonia et al., "Fetal electrocardiograms, direct and abdominal with reference heartbeat annotations," Sci. Data, vol. 7, p. 200, 2020.
- [15] W. Qian et al., "Continuous transabdominal fetal pulse oximetry (TFO) in pregnant ewe models under induced fetal hypoxia," Amer. J. Obstet. Gynecol., vol. 228, no. 1, p. S242–243, 2023.
- [16] B. Kasap et al., "KUBAI: Sensor fusion for non-invasive fetal heart rate tracking," *IEEE Trans. Biomed. Eng.*, 2023.